Hindawi
International Journal of Aerospace Engineering
Volume 2019, Article ID 7693403, 13 pages
https://doi.org/10.1155/2019/7693403

Research Article

Failure Analysis of the Pin Bore of the Combined Piston for the Aero Engine

Zhongjian Pan[1,2,3] **and Lei Guo**[1]

[1]*School of Mechanical and Electronic Engineering, Changsha University, Changsha, 410022 Hunan, China*
[2]*Sunward Intelligent Equipment Co., Ltd., Changsha, 410100 Hunan, China*
[3]*School of Mechanical and Electronic Engineering, Central South University, Changsha, 410083 Hunan, China*

Correspondence should be addressed to Zhongjian Pan; pzjian1005@163.com

Received 16 July 2019; Revised 6 October 2019; Accepted 17 October 2019; Published 21 December 2019

Academic Editor: Linda L. Vahala

The combined piston can be used in an aero piston heavy fuel engine because of its light weight, so as to reduce the reciprocating inertia force and improve the engine power-weight ratio. However, the pin bore of the combined piston is prone to deform leading to the failure of the piston. Based on the structure of the piston, the stress of the piston under thermomechanical coupling is analyzed, the temperature field of the piston is determined by experiments, and the deformation rule of the piston pin bore under the thermomechanical coupling is summarized. A design scheme is proposed to change the position of the thread connection between the piston crown and the piston head. Under the same conditions, the deformation of the piston pin bore of the original scheme and the new scheme is analyzed. The results show that together with the changing of the connection thread between the piston crown and the piston head, the deformation of the piston pin bore decreases by 60 μm and the deformation of the piston pin bore is controlled. The test results show that the deformation of the pin bore is within the acceptable range, which proves the effectiveness of the improved scheme.

1. Introduction

Because of the military's single standard on fuel and the economy and availability for civil use, the compression ignition aviation piston engine has become a hot research topic [1]. Compared with jet engines, compression ignition piston-propeller aircraft has better fuel economy [2], low noise [3], emission, and easy maintenance. The unmanned aerial vehicle (UAV) needs a long hovering time; the engine is required to have high fuel economy, but the jet engine cannot meet this requirement. Civil piston propeller aircraft are used for pilot training, rescue, private flight, etc. Pilots want to use an economical and available fuel [4, 5]; all these have promoted the development of the aviation diesel engine. At present, a general aircraft mainly uses aviation gasoline engines, compression ignition aviation heavy fuel engines are used less, and there are very few reports on their research [6, 7]. To reduce the weight of the piston, lower the piston inertia force during the reciprocating process, and improve the power-weight ratio, some aviation piston compression ignition engines adopt a combined piston with the head made of high strength steel and piston skirt of aluminum alloy. But the lightweight problem is not the main focus of this paper; the combined piston consists of two parts. The inhomogeneous material properties and the defect of the structure design will lead to piston fatigue. At present, the combined piston is mainly used in automobile engines, which has hardly been used in an aviation piston engine. Rebhi et al. have studied the key components of the aircraft engine, such as the cylinder head; observed and analyzed fatigue cracks; confirmed that the crack origin was located at the most stressed area; and done a lot of research work on fatigue lifetime in terms of material properties of aircraft and engine components [8]. These studies are of great significance for improving the life of engine components or the reliability of aircraft systems. They focus on the finite element theory without changing the internal structure of components, but the research methods can be used for reference

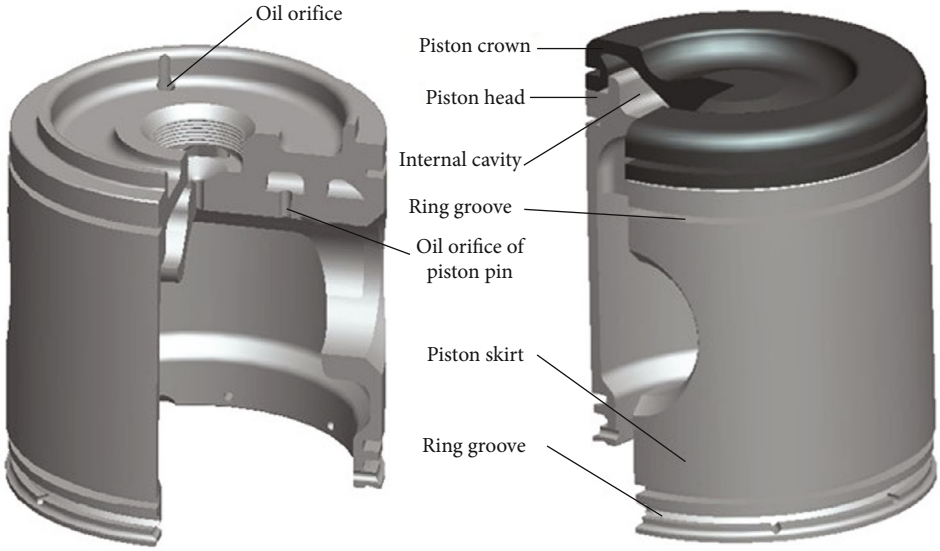

Figure 1: Internal structure of the combined piston.

in the fatigue analysis of the combined piston [9–11]. Liu et al. has researched the relationships between the piston life and stress in different thermal, mechanical, and thermal-mechanical coupling conditions, but the integral piston studied by the authors is not a combined piston. The internal structure of the combined piston is different from the integral piston, and the stress and deformation of both pistons are different under the same conditions [12]. Ijaz et al. has researched a comprehensive delamination crack growth mathematical model under fatigue loading, but it is suitable glass fibre-reinforced plastic composite laminates [13]. Yu et al. has researched that the appearance of longitudinal inclusion clusters of excess size in the crack origin zone is mainly responsible for the failure of the piston pin and improvement of steel purity is suggested to prevent future piston pin failures [14]. Most scholars have done a lot of research on the deformation of piston skirts and piston pins; these studies are not closely related to the combined piston [15, 16] or improve piston performance by adding a coating to the piston crown for preventing piston deformation; these improvements have nothing to do with the internal structure of the piston [17, 18], but there are few reports on the research of the pin bore of combined pistons. The type certification of the aviation piston engine has always been restricted by the reliability of the piston, which has become a major obstacle to the development of the power of general aviation aircraft. Based on the deformation of the combined piston pin bore of a developing aviation piston heavy fuel engine as the research object, the paper analyzes the internal structure of the combined piston; also, the rule between the deformation of the piston pin bore and the position of internal thread is studied under the conditions of cylinder pressure, mechanical load, side force, and other multifield coupling. What is more, a new solution is also provided to solve the technical problem of the deformation of the combined piston pin bore. The proposed design scheme can improve the reliability of the engine piston and greatly shorten the time for the engine to obtain airworthiness certification. At present, some research institutes are developing aero diesel engines and some companies are researching a combined piston for marine 2-stroke diesel engines and 4-stroke automotive diesel engines, which can be used for reference by these institutes. It can even be derived to a similar combined structure design to provide ideas for structural optimization design.

2. Internal Structure and Failure Description of the Combined Piston

It is more suitable to use forged steel for the piston because this type of engine uses kerosene or diesel as fuel which has a large explosion pressure in the cylinder and high combustion temperature. However, the aviation piston engine has strict requirements on weight. So, it needs to reduce the weight of the piston as much as possible and also to reduce the inertia force of the piston in high-speed reciprocating motion. For this reason, the piston adopts a combined design which means the piston crown is made of forged steel while the piston skirt is made of aluminum alloy connected by a thread. The piston structure is shown in Figure 1.

A large amount of deformation on the piston pin bore occurs when the engine is having endurance testing. The value is 0.06 mm and more than what manufacturers allow. The gap between the pin bore and pin leads to a strong impact of the piston in high-speed reciprocating motion, which further aggravates the deformation of the piston and pin bore, until the engine cannot work properly, affecting flight safety.

3. Simulation Analysis under the Condition of Thermomechanical Coupling

In order to analyze the deformation of the combined piston pin bore, simulation analysis is carried out. According to the boundary conditions, the deformation law of the piston pin bore is summarized and the modification scheme is proposed.

Table 1: Mechanical performance parameters of piston components.

Name	Yield strength (MPa)	Tensile strength (MPa)	Elasticity modulus (GPa)	Thermal conductivity (W/(m·K))	Coefficient of linear thermal expansion (M/(m·K))	Poisson ratio
Piston crown	≥205	≥520	206	16.3	17.5×10^{-6}	0.31
Piston skirt	≥152	≥251	71	163	23.9×10^{-6}	0.33

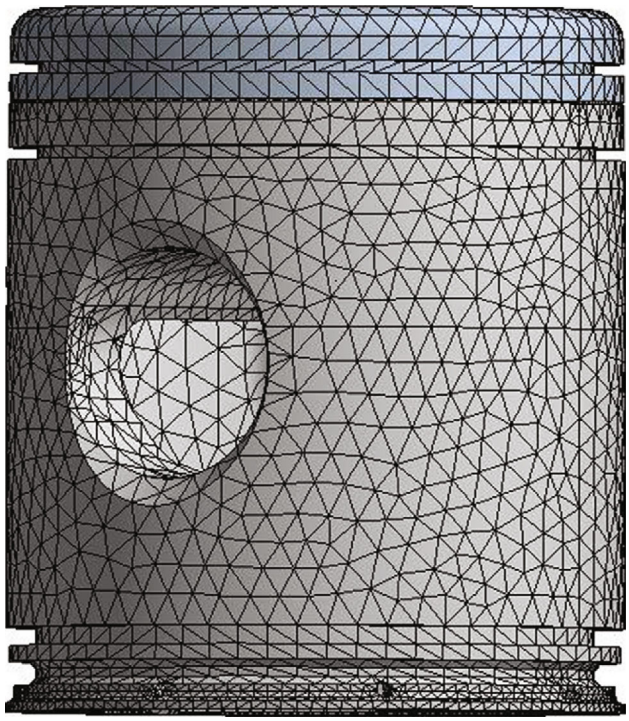

Figure 2: The meshing of the piston.

3.1. Mechanical Performance Parameters and Meshing. Before numerical simulation analysis, the material of the piston crown and the piston skirt needs to be defined in order to provide accurate conditions in finite element analysis. Mechanical performance parameters of the piston components are shown in Table 1.

After the 3D model is established, the finite element analysis software is introduced to conduct grid division. Because the quadratic tetrahedron unit has the same calculation accuracy as the hexahedron unit, there is a smaller bandwidth matrix and shorter calculation time. Besides, it can adaptively partition the structure of special location and automatically implement grid encryption. Therefore, quadratic tetrahedron units are used and division results are shown in Figure 2.

3.2. The Application of Boundary Conditions. The accuracy of boundary conditions is directly related to the results of numerical simulation, which directly affects the analysis of engineering problems. Therefore, precise boundary conditions are required before numerical simulation. For the boundary conditions of the piston, mechanical stress load and temperature field are the main factors.

3.2.1. The Mechanical Stress Load Curve of the Piston. The main forces acting on the piston are the gas pressure acting on the piston crown and the side force acting on the piston skirt. Other forces are relatively small and have little influence on the overall deformation of the piston pin bore which are not taken into account.

(1) Cylinder Pressure Acting on the Piston Crown. Through the simulation software, the gas pressure curve of the piston crown at the maximum speed of the engine is obtained, and the experimental value is compared with the simulation value to verify the correctness of the simulation curve. Shown in Figure 3 is the maximum force curve on the piston.

(2) The Side Force Acting on the Piston. The side force of the piston is produced in both the compression stroke and the power stroke. When the piston is doing work, the main thrust surface is subjected to side force. While the piston is compressed, the secondary thrust surface is subjected to side force. The side thrust curve of each piston in a period is shown in Figure 4 with the maximum side force of 5182 N and the maximum secondary thrust of -2489 N.

3.2.2. Temperature Field Measurement and Numerical Simulation. Temperature field and heat transfer coefficient are important boundary conditions for the piston thermal analysis [19, 20]. The third type of boundary condition is usually adopted in the analysis of the piston, which requires the temperature T and heat transfer coefficient α of the peripheral medium to be given. The G. Eichelberg formula is usually selected to calculate it [21]. The experiment can be conducted after calculating the heat transfer coefficient and temperature field [22]. Then, the actual temperature field on the piston surface is measured and the heat transfer coefficient is constantly revised until the measured value is basically consistent with the actual value.

$$\alpha_g = 7.699\sqrt{p_g T_g} \cdot \sqrt[3]{C_m}, \tag{1}$$

where p_g is the instantaneous pressure of gas, MPa; T_g is the instantaneous temperature of gas, K; and C_m is the average velocity of the piston, m/s.

The hardness plug method is commonly used to measure the temperature field of the piston, which has little influence on the temperature distribution and the piston strength and also is easy to operate. The hardened temperature plug material is made into screws which are screwed into the area to be measured. Then, the engine runs 2 hours under the condition of a fatigue endurance test and then stops after cooling.

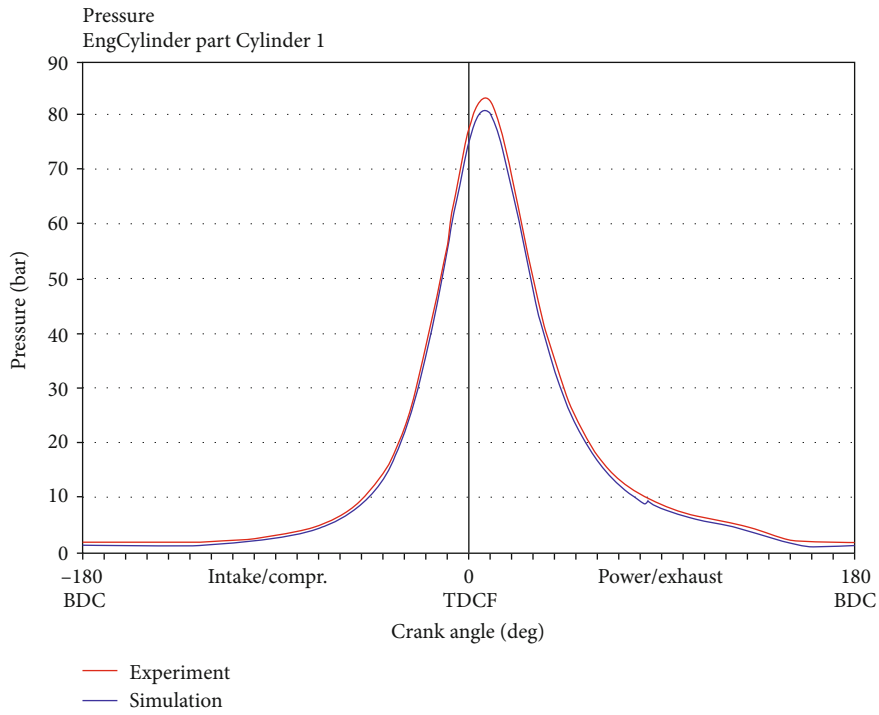

Figure 3: Cylinder pressure curve at 2700 r/min.

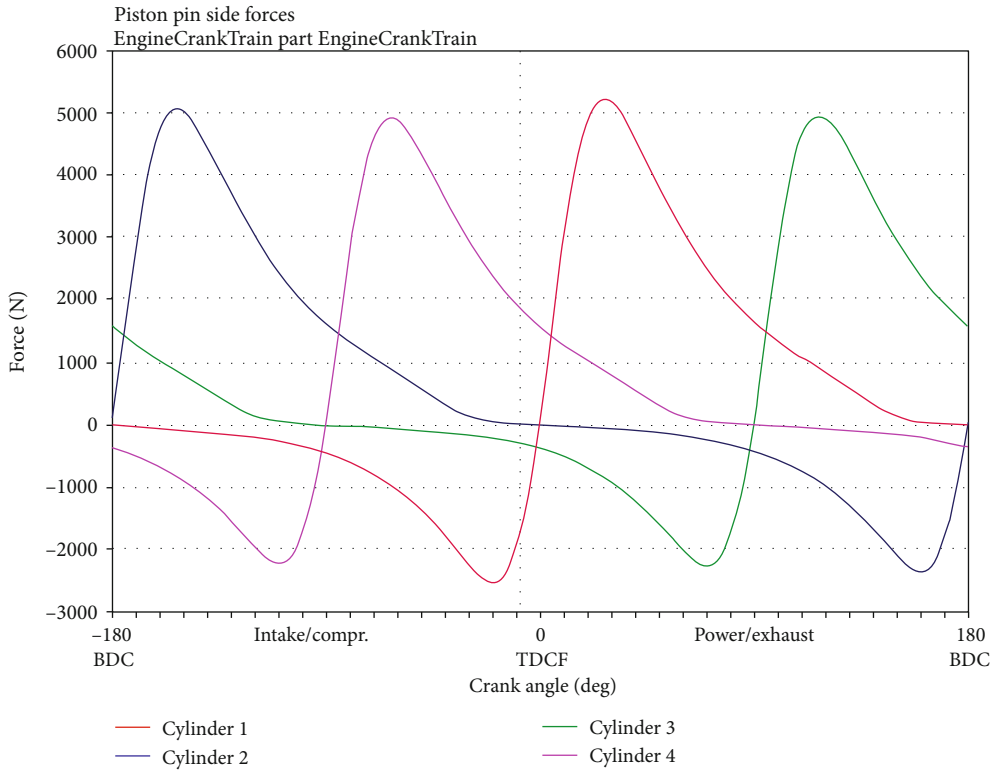

Figure 4: Piston pin side force curve at 2700 r/min.

Afterwards, the hardness plug is removed and the hardness is measured by a micro hardness tester after polishing. The temperature found correspondingly to relationship curves between hardness and temperature is the measured value. The installation of the experimental measurement point is shown in Figure 5.

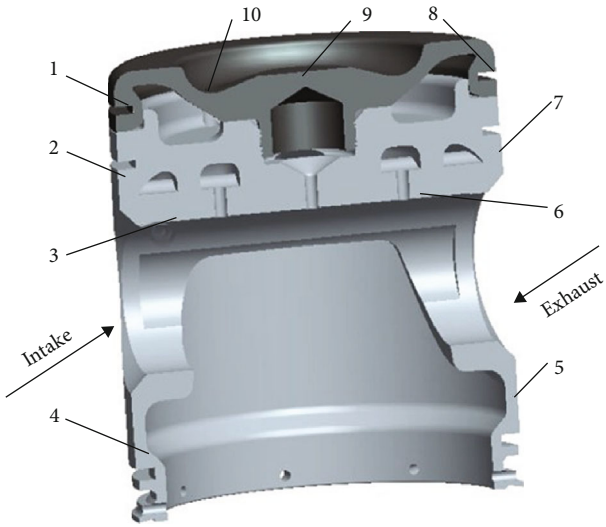

Figure 5: Mounting position of plug on the piston.

After the experiment, the hardness screws should be removed shortly after the engine stops. At the time, the piston is still hot and the hardness screws are not yet gummed. The hardness plug is taken out by professional fixture, and its end surface is polished. Only one person should measure the reading to reduce the measurement error. The temperature is determined according to the measured hardness value and cooling time.

The data of several important parameter points in the experiment are recorded as shown in Table 2.

The comprehensive heat transfer coefficient of the piston is modified according to the measured value of the piston, and the thermal boundary conditions under the condition of 2700 r/min are obtained as shown in Table 3.

Based on simulation through the above boundary conditions, numerical simulation is carried out on the piston in the Workbench. We entered the ambient temperature and the convective heat transfer coefficient in Table 3 successively into each face, and the piston temperature field calculation results are obtained as shown in Figure 6.

The analysis results of the piston temperature field show that the maximum temperature of the piston crown is 530.6°C and of the combustion chamber bottom is 498.4°C. The temperature of the fire shore is 384.7°C; the lowest temperature of the piston skirt is 116°C. The simulation result of the whole temperature field is not far from the actual measurement result, which verifies the accuracy of the numerical simulation and provides a reliable theoretical analysis basis for the subsequent scheme optimization. Meanwhile, it is known from Figure 7 that the temperature of the measuring point 2 below the first ring groove is lower than that of point 7 in the exhaust side. The numerical results are 148.2°C and 176.4°C. This is because the engine uses piston scavenging; the cold air entering from the intake port plays a certain cooling role on the piston. While the temperature of measuring point 3 in the piston pin bore is close to that of measuring point 6, which are 164.3°C and 169.6°C, respectively, both measuring points are inside the piston and the temperature distribution is even. Among these, the simulation value of point 3 is close to the measured value while the temperature of point 6 is 12°C or so lower than the actual temperature, with some error.

3.3. Simulation Analysis. Mechanical stress is added separately in the analysis including gas pressure, side thrust, and other main loads. Generally speaking, mechanical stress and strain are the main factors of piston pin bore deformation. The force and the deformation of the piston pin bore under simple mechanical load are considered. In addition, thermal stress is added to simulate thermal coupling of the engine, and the force and the deformation of the piston pin bore are comprehensively observed under the condition of the joint action of the thermomechanical stress field.

Figures 8 and 9 show the main deformation and stress nephogram of the piston under mechanical stress. Under the action of simple mechanical stress, the maximum stress of the piston is on both sides of the pin bore and the maximum stress is 208 MPa. This is mainly because the transition angle between both sides of the piston pin bore and the piston skirt intersection is not big enough, resulting in local stress concentration. The maximum stress produced on the piston pin bore upper surface is 105.2 MPa, while the stress of the piston skirt is even lower than the stretch limit of the material. This is because the gas pressure transfers the force to the piston pin through the upper surface of the piston pin bore; the piston pin bore is under great pressure in the whole engine cycle work. Therefore, the whole piston under the action of mechanical stress is safe.

The maximum deformation of the whole piston is 0.044 mm under the action of simple mechanical stress and mainly at the piston pin bore, which indicates that the piston is deformed under the combined action of gas pressure, side thrust, friction, and other stresses. Besides, the deformation value exceeds the maximum allowable deformation value of the piston pin bore. In many stress fields, gas pressure plays a leading role in the deformation of the piston pin bore.

Thermal stress is added to analyze the stress and the strain of the piston and the pin bore under the thermal-mechanical coupling, as shown in Figures 10 and 11. The piston is fully dissected, and the deformation nephogram is enlarged by 50 times; it is found that the maximum deformation of the piston occurs at the periphery of the piston crown reaching 0.23 mm. This indicates that the temperature field has an important influence on the deformation of the piston head.

There is almost no deformation at the pin bore because the female thread of the middle area of the piston head is connected with the male thread of the piston head. The tip of the piston expands at the edge due to thermal stress.

The minimum deformation value is 0.065 m at the middle position of the piston pin bore while it increases 0.021 mm under the simple mechanical stress, which means that thermal stress has little effect on pin bore deformation.

The maximum stress of the piston is 359 MPa. It mainly occurs at the piston crown, which indicates that the temperature field plays a major role in the stress change here; high temperature affects mechanical properties of metals. The maximum stress at the piston pin bore is 168 MPa, which

Table 2: Test values of piston temperature field.

Number	1	2	3	4	5	6	7	8	9	10
Measured value (°C)	391	153	162	132	141	181	178	394	530	490

Table 3: The third kind of thermal boundary condition of the piston of an aircraft engine.

Position	Ambient temperature (K)	Convective heat transfer coefficient (W/(m^2·K))	Position	Ambient temperature (K)	Convective heat transfer coefficient (W/(m^2·K))
Piston crown	700	503	Upper part of piston cavity	360	310
Piston bank	450	98	Lower part of piston cavity	360	290
Piston skirt	160	300	Oil passage	230	480
Pin bore	210	270	Upper first ring groove	430	700
Other ring grooves	200	250	Lower first ring groove	400	650

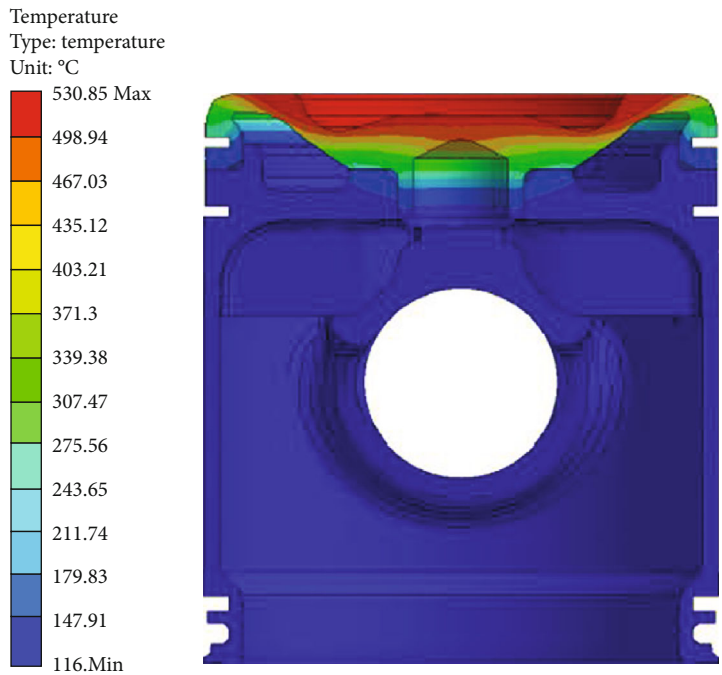

Figure 6: Overall temperature distribution of the piston.

increases 65 MPa compared with the simple mechanical stress. Therefore, the main deformation at the piston pin bore is mainly caused by mechanical stress.

4. The Optimization Scheme Is Proposed and Analyzed

4.1. The Optimization Scheme Is Proposed. The above description shows that the high temperature of the combustion chamber is the main cause of the deformation of the piston pin bore. Moreover, the material properties of the piston crown and the piston skirt are different, which leads to the deformation of the piston pin bore together with the combustion chamber after thermal expansion. The design changes are shown in Figures 12 and 13. The position of the direct connection thread between the piston crown and the piston head is modified, as shown in the original design and the new design.

4.2. Comparative Analysis of Simulation

4.2.1. Comparison of Pin Bore Deformation. Local structure is modified without changing the overall structure based on the theoretical analysis and comparison with the existing piston structure. It is hoped that the deformation of the pin bore can be reduced to the permissible clearance range of the engine assembly. Applying the same load, the two schemes

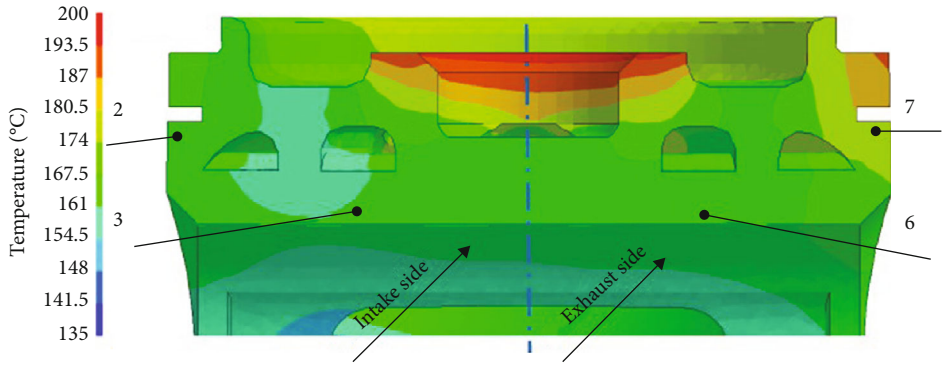

Figure 7: The temperature distribution of the piston head.

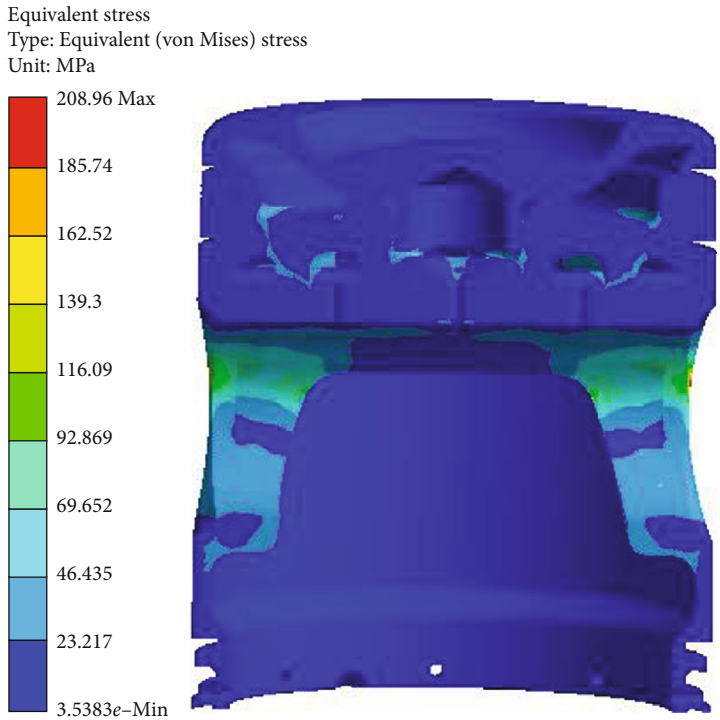

Figure 8: The von Mises stress nephogram of the piston under mechanical stress condition.

are compared and the number of cycles is set at 2.3×10^7. The simulation results are shown in Figure 14.

Figure 14 is the comparison of the deformation amount of the piston pin bore before and after changing the position of the connecting thread. It can be seen from the analysis that the deformation amount of the pin bore changes when the connection position of the screw thread changes, which is greatly reduced compared with the original design. Take A and B on both sides of the pin bore as standard and the generatrix on the pin bore as the research object to measure its deformation value. When it is of the original connection mode, the deformation amount of the pin bore is shown in Figure 14 on the left. Taking slice A and slice B as standard, the maximum deformation amount is 0.06 mm. When the thread connection position changes, the deformation of the pin bore is shown in Figure 14 on the right. Also, taking A and B as standard, the maximum deformation is 0.01 mm and reduces by 83.3%, the pin bore deformation is greatly reduced, and the reliability of engine operation is improved. If the deformation value exceeds the maximum deformation range, the piston will deviate or even knock the cylinder during reciprocating movement. Therefore, the deformation of the pin bore plays an important role in the normal operation of the piston. The change of the position of the connecting thread has a good effect on restraining the deformation of the pin bore.

Before and after changing the position of the connecting thread, the deformation of A and B surfaces on both sides of the pin bore also changes greatly. When the original connection is made, the deformation of A and B is shown

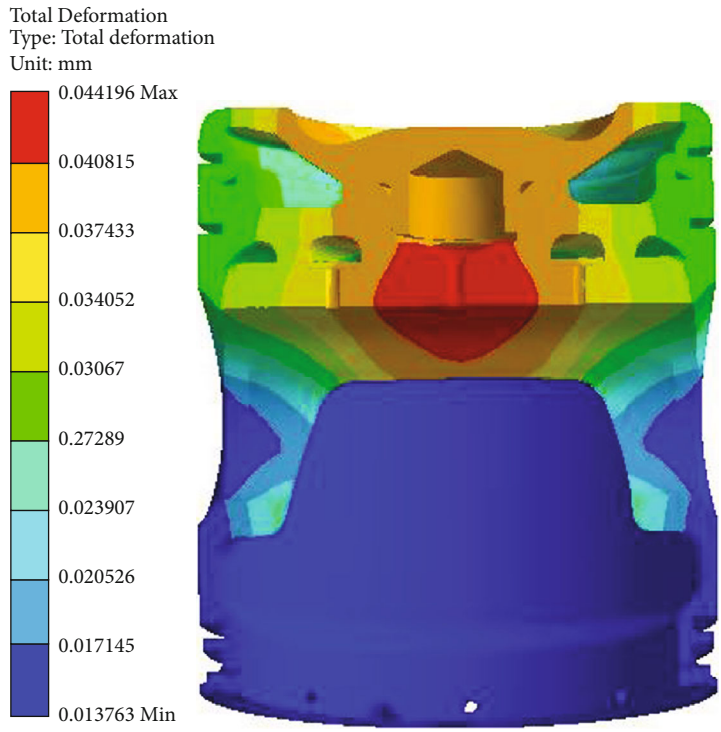

Figure 9: The deformation nephogram of the piston under mechanical stress condition.

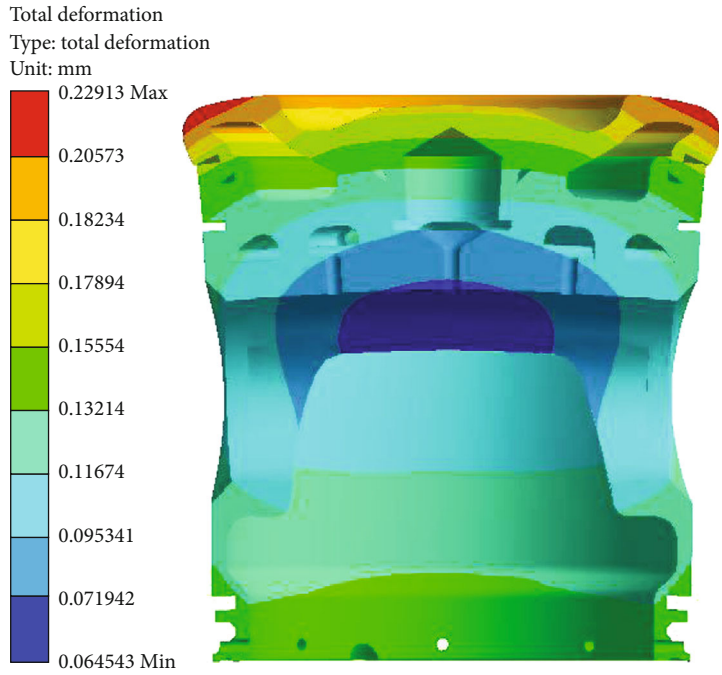

Figure 10: The deformation nephogram of the piston under thermomechanical stress coupling condition.

by the red line in Figure 14. Friction between the pin and the pin bore leads to an oval shape on A and B of the pin bore. When the new design scheme is adopted, the deformation of A and B has been greatly improved compared with the previous one. As shown by the blue line in Figure 14, the deformation of A and B no longer presents an oval shape but a regular round shape. The radius value of B is about 0.002 mm larger than A, which is mainly because the stress on main force surface is different from the thrust surface under the reciprocating piston effect.

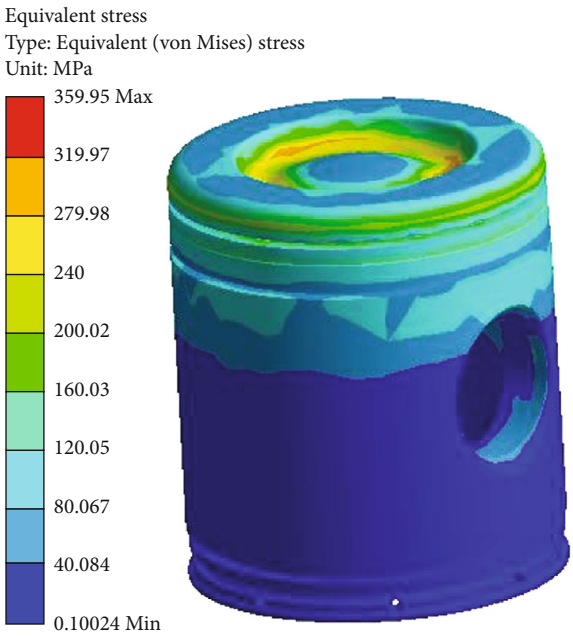

Figure 11: The von Mises stress nephogram of the piston under thermomechanical stress coupling condition.

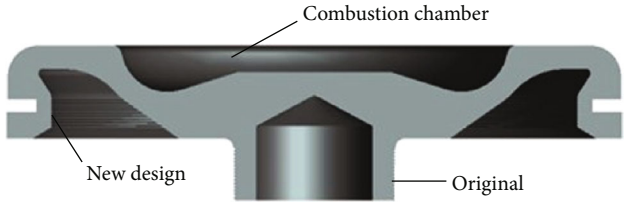

Figure 12: Two schemes for thread connection.

However, the difference is acceptable because of its small impact on the engine.

4.2.2. The Overall Deformation Analysis. After analyzing the deformation of the piston pin bore, the deformation of the whole piston before and after changing the thread position is observed and compared. By applying the same boundary conditions, the stress and deformation of the piston assembly and the piston pin bore are observed under the combined action of temperature field and mechanical stress, as shown in Figures 15 and 16.

The maximum stress at the piston crown changes from 359.95 MPa to 472.74 MPa, increasing 32.17% after the improvement. The maximum stress area is transferred from the bottom of the combustion chamber to the point where the fire bank meets the first ring groove. This is mainly because the top of the combustion chamber is losing constraints and the entire piston crown is acting upwards under the action of thermal stress and reciprocating inertia force after changing the connecting position, then larger stress is produced in the weak junction. Because the stress is still less than the tensile strength of the piston material, it is still within the safety range.

The maximum stress at the piston pin bore does not change much at 173.5 MPa, which is slightly less than the 168 MPa before the improvement, indicating that the pin bore was mainly affected by gas pressure.

The new design has great influence on the overall deformation of the piston. The current maximum deformation is 0.236 mm, which only increases 0.007 mm from 0.229 mm before the improvement. Moreover, the position where maximum deformation is taking place basically does not change. However, it plays an important role in restraining the deformation of the piston pin bore.

5. The Experiment

The piston assembly is manufactured according to the modified scheme. Before the test, the size of the piston pin is measured. The outer diameter of the piston pin is 38.102 mm, and the inner diameter is 38.110 mm. The single piston fatigue test is difficult for simulating the boundary conditions of piston analysis and cannot reflect the real working conditions of the piston. Therefore, the endurance test of the piston pin bore is carried out together with the engine endurance test. The piston is installed on the engine for fatigue endurance testing and is tested in the same environment. External test conditions are shown in Table 4.

The endurance test of the engine needs to be carried out on the bench test; propellers must be installed on the bench as shown in Figure 17, and this is different from other parts that can be fatigue tested independently. The bench can measure the torque and thrust and monitor the operating parameters of the engine. According to the requirements of the engine endurance test, the endurance test for 150 hours is completed according to the 14CFR33 of Federal Aviation Administration (FAA) [23]:

(1) A 30-hour run consisting of alternate periods of 5 minutes at rated take off power and 5 minutes at maximum recommended cruising power

(2) A 20-hour run consisting of alternate periods of 1.5 hours at rated maximum continuous power and 0.5 hour at 75% maximum continuous power and 91% maximum continuous speed

(3) A 20-hour run consisting of alternate periods of 1.5 hours at rated maximum continuous power and 0.5 hour at 70% maximum continuous power and 89% maximum continuous speed

(4) A 20-hour run consisting of alternate periods of 1.5 hours at rated maximum continuous power and 0.5 hour at 65% maximum continuous power and 87% maximum continuous speed

(5) A 20-hour run consisting of alternate periods of 1.5 hours at rated maximum continuous power and 0.5 hour at 60% maximum continuous power and 84.5% maximum continuous speed

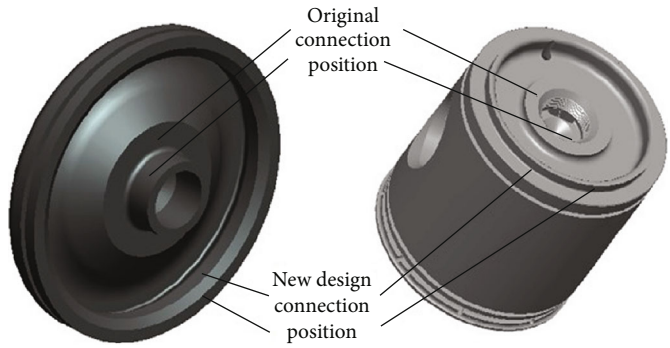

Figure 13: Original design and new design for connection position.

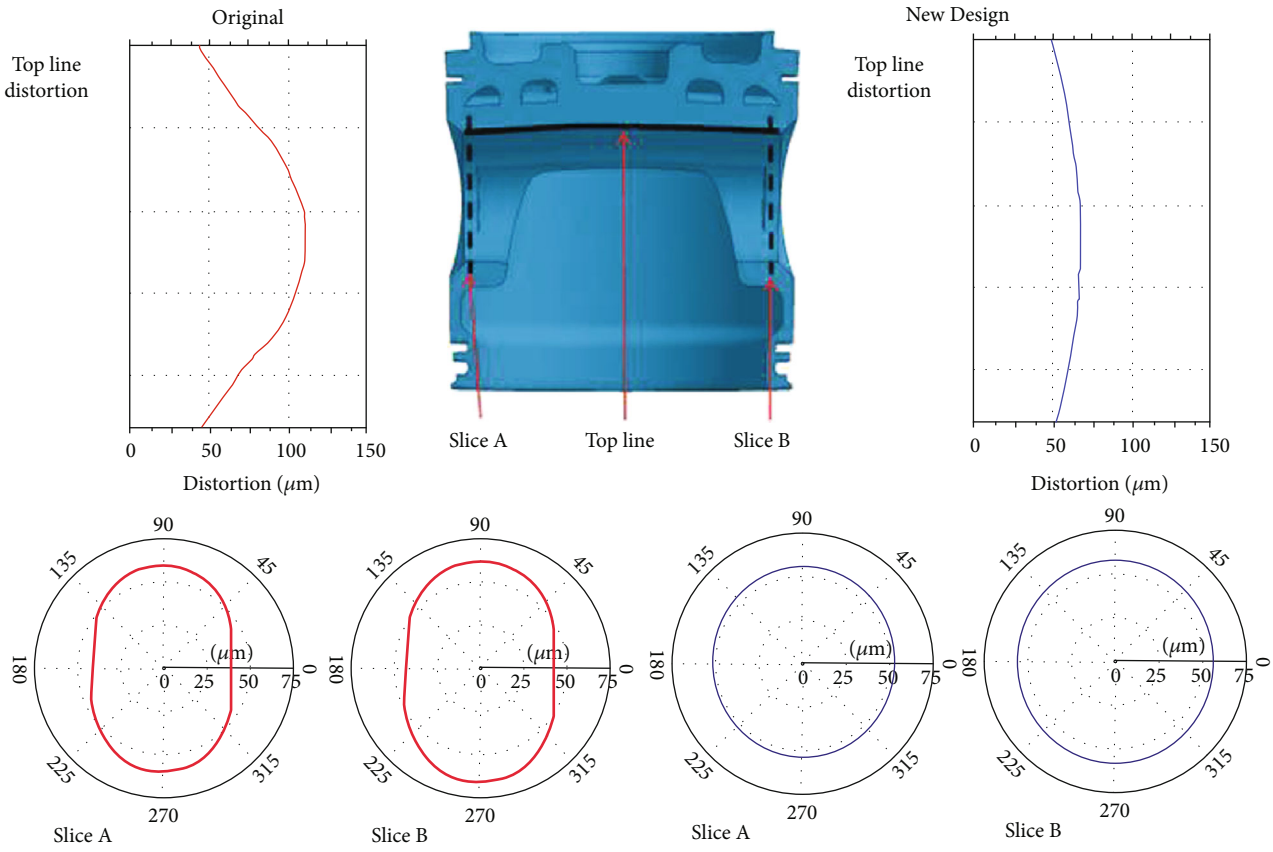

Figure 14: The comparison of deformation amount of the piston pin bore between the original design and the new design.

(6) A 20-hour run consisting of alternate periods of 1.5 hours at rated maximum continuous power and 0.5 hour at 50% maximum continuous power and 79.5% maximum continuous speed

(7) A 20-hour run consisting of alternate periods of 2.5 hours at rated maximum continuous power and 2.5 hours at maximum recommended cruising power

The engine is tested for 150 hours under the above conditions, and various parameters of the engine are recorded to ensure the normal operation of the engine. When the engine finishes running, the engine is dismantled after the machine is cooled to check the inner diameter of the piston pin holder and the outer diameter of the piston pin.

After the removal, abrasions or cracks inside of the pin bore and the surface of the piston pin are firstly checked from the outside. Then, the outside diameter of the piston pin is measured with the outside micrometer, and the average value is 38.098 mm obtained after measuring several times. Thirdly, the piston pin bore is measured with the inside micrometer mainly for the inner diameter of the middle section of the piston pin bore. The average value is 38.121 mm after multiple measurements. All the deformation values of the piston pin and the pin bore are within the limits of a manufacturer's deformation requirement.

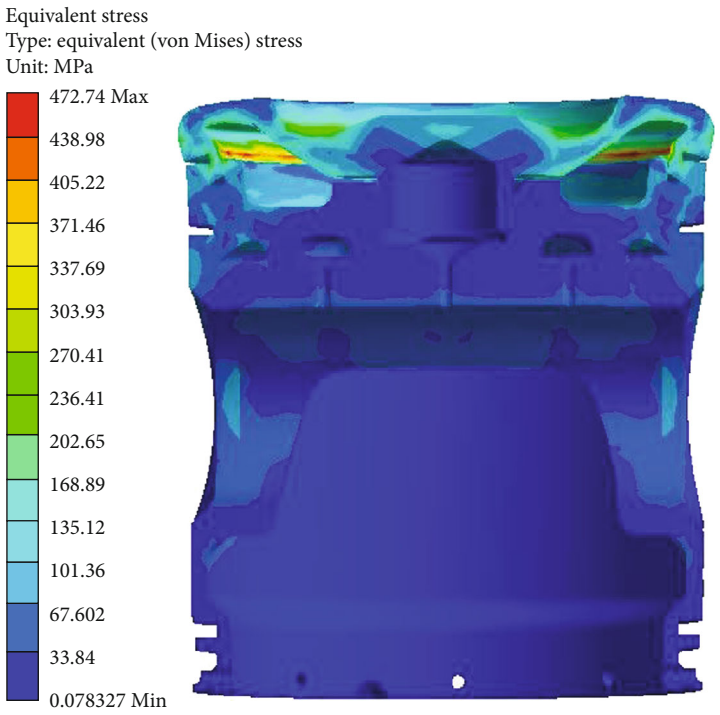

Figure 15: The von Mises stress nephogram of the piston under the new scheme condition.

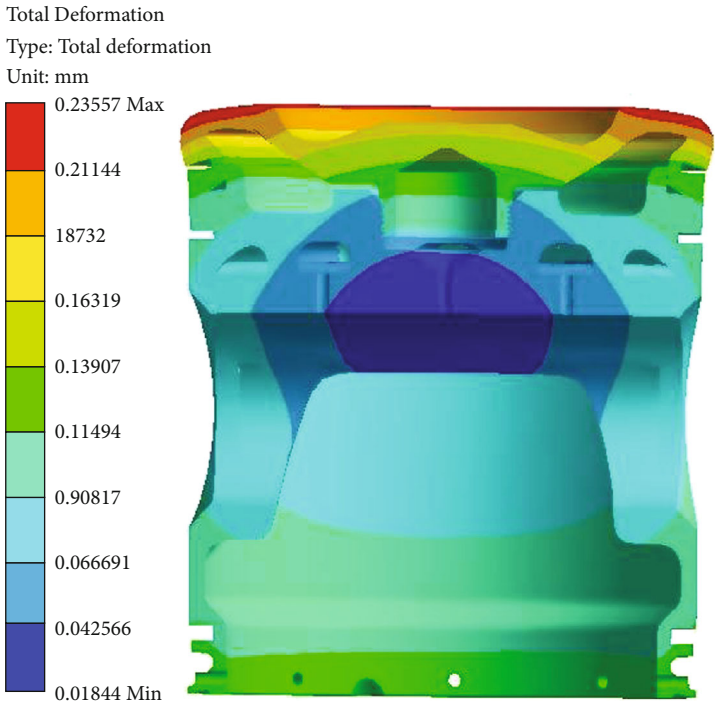

Figure 16: The deformation nephogram of the piston under new scheme condition.

6. Conclusions

In this paper, pin bore fatigue of the combined piston is studied. The composition of the combined piston is analyzed, and the boundary conditions of the piston analysis are discussed. The reliability of the piston is improved by changing the connecting position of internal threads of the piston, and the piston fatigue problem caused by pin bore deformation is solved. The conclusions are as follows:

Table 4: Engine test conditions.

Ambient temperature	20°C
Atmospheric pressure	968 kPa
Engine RPM (r/min)	Endurance test requirements
Engine run-up time (h)	≥150
Oil pressure (bar)	3-8 bar
Oil temperature (°C)	50-110
Coolant temperature (°C)	80-120

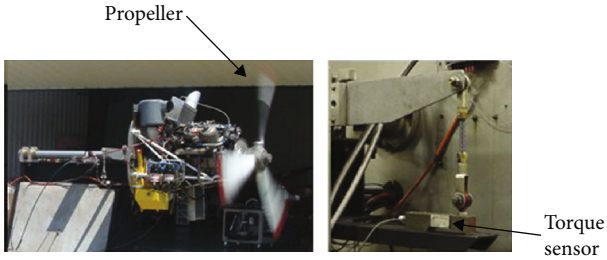

Figure 17: The engine endurance test.

(1) Different material properties of the combined piston have influence on the deformation of the piston pin bore

(2) Changing the connecting position of the internal threads of the piston can reduce the deformation of the pin bore of the piston

(3) The reliability of the piston directly affects the operation of the engine. It is necessary to carry out reliability experiments with the engine in order to ensure that the piston can be adequately verified under real working conditions

Data Availability

The simulation and experimental data used to support the findings of this study are included within the article. The pin bore of the combined piston simulation data have been recorded in the manuscript, and the bench test data is also recorded and analyzed in the manuscript, which proves the effectiveness of the improved scheme. The figures and tables in the manuscript record the data in detail, such as Table 1 which shows the mechanical performance parameters of piston components, Table 2 which shows the test values of the piston temperature field, and Figures 6–16 which record the simulation data.

Conflicts of Interest

There is no conflict of interest regarding the publication of this article.

Acknowledgments

The research leading to these results has received funding from the project supported by the scientific research of the Hunan Provincial Education Department under grants 18C0776 and 16B029, Changsha Science and Technology Bureau under grant K1705041, and Hunan Provincial Natural Science Foundation under grant 2019JJ50684. Last but not the least, the authors are thankful to the director for permission to publish this work.

References

[1] A. K. Sehra and W. Whitlow Jr., "Propulsion and power for 21st century aviation," *Progress in Aerospace Sciences*, vol. 40, no. 4–5, pp. 199–235, 2004.

[2] Z. Pan, Y. Deng, and L. Cheng, "Regular analysis of aero-diesel piston engine between combustion chamber size and emission," *International Journal of Aerospace Engineering*, vol. 2019, 12 pages, 2019.

[3] A. T. Wall, K. L. Gee, M. M. James, K. A. Bradley, S. A. McInerny, and T. B. Neilsen, "Near-field noise measurements of a high-performance military jet aircraft," *Noise Control Engineering Journal*, vol. 60, no. 4, pp. 421–434, 2012.

[4] D. Cirigliano, A. M. Frisch, F. Liu, and W. A. Sirignano, "Diesel, spark-ignition, and turboprop engines for long-duration unmanned air flights," *Journal of Propulsion and Power*, vol. 34, no. 4, pp. 878–892, 2018.

[5] Z. Pan, Q. He, X. Zhang, and D. Zhang, "Numerical simulation of 2-stroke diesel engine for light aircraft," *IEEE Aerospace and Electronic Systems Magazine*, vol. 30, no. 3, pp. 4–10, 2015.

[6] A. P. Carlucci, A. Ficarella, D. Laforgia, and A. Renna, "Supercharging system behavior for high altitude operation of an aircraft 2-stroke diesel engine," *Energy Conversion and Management*, vol. 101, pp. 470–480, 2015.

[7] Z. Pan and Q. He, "High cycle fatigue analysis for oil pan of piston aviation kerosene engine," *Engineering Failure Analysis*, vol. 49, pp. 104–112, 2015.

[8] L. Rebhi, B. Krstic, A. Boutemedjet et al., "Fatigue fracture analysis of an ADF antenna in a military aircraft," *Engineering Failure Analysis*, vol. 90, pp. 476–488, 2018.

[9] S. K. Bhaumik, M. Sujata, and M. A. Venkataswamy, "Fatigue failure of aircraft components," *Engineering Failure Analysis*, vol. 15, no. 6, pp. 675–694, 2008.

[10] B. Krstic, L. Rebhi, D. Trifkovic et al., "Investigation into recurring military helicopter landing gear failure," *Engineering Failure Analysis*, vol. 63, pp. 121–130, 2016.

[11] X. Xue, S. Wang, J. Yu, and L. Qin, "Wear characteristics of the material specimen and method of predicting wear in floating spline couplings of aero-engine," *International Journal of Aerospace Engineering*, vol. 2017, Article ID 1859167, 11 pages, 2017.

[12] X. F. Liu, Y. Wang, and W. H. Liu, "Finite element analysis of thermo-mechanical conditions inside the piston of a diesel engine," *Applied Thermal Engineering*, vol. 119, pp. 312–318, 2017.

[13] H. Ijaz, W. Saleem, M. Zain-ul-abdein, A. A. Taimoor, and A. S. B. Mahfouz, "Fatigue delamination crack growth in GFRP composite laminates: mathematical modelling and FE simulation," *International Journal of Aerospace Engineering*, vol. 2018, Article ID 2081785, 8 pages, 2018.

[14] Z. Yu, X. Xu, and H. Ding, "Failure analysis of a diesel engine piston-pin," *Engineering Failure Analysis*, vol. 14, no. 1, pp. 110–117, 2007.

[15] Y. Hamid, A. Usman, S. K. Afaq, and C. W. Park, "Numeric based low viscosity adiabatic thermo-tribological performance analysis of piston-skirt liner system lubrication at high engine speed," *Tribology International*, vol. 126, pp. 166–176, 2018.

[16] I. Etsion, G. Halperin, and E. Becker, "The effect of various surface treatments on piston pin scuffing resistance," *Wear*, vol. 261, no. 7–8, pp. 785–791, 2006.

[17] B. Zabala, A. Igartua, X. Fernández et al., "Friction and wear of a piston ring/cylinder liner at the top dead centre: experimental study and modelling," *Tribology International*, vol. 106, pp. 23–33, 2017.

[18] N. Sergent, M. Tirovic, and J. Voveris, "Design optimization of an opposed piston brake caliper," *Engineering Optimization*, vol. 46, no. 11, pp. 1520–1537, 2014.

[19] M. Cerit and M. Coban, "Temperature and thermal stress analyses of a ceramic-coated aluminum alloy piston used in a diesel engine," *International Journal of Thermal Sciences*, vol. 77, pp. 11–18, 2014.

[20] E. Gingrich, J. Ghandhi, and R. D. Reitz, "Experimental investigation of piston heat transfer in a light duty engine under conventional diesel, homogeneous charge compression ignition, and reactivity controlled compression ignition combustion regimes," *SAE International Journal of Engines*, vol. 7, no. 1, pp. 375–386, 2014.

[21] T. L. Hendricks, D. A. Splitter, and J. B. Ghandhi, "Experimental investigation of piston heat transfer under conventional diesel and reactivity-controlled compression ignition combustion regimes," *International Journal of Engine Research*, vol. 15, no. 6, pp. 684–705, 2014.

[22] Y. Jin, D. Wang, and B. Wen, "Dynamic simulation on double-rotor system of aero-engine with rubbing fault," *Journal of Harbin Engineering University*, vol. 38, no. 12, pp. 1872–1876, 2017.

[23] https://www.faa.gov/regulations_policies/faa_regulations/.